

# Preliminary seismic analysis and strengthening proposals of two churches in Azores

Aníbal Costa, António Arêde, Domingos Moreira & Nuno Neves  
*Faculty of Engineering at Porto University, Porto, Portugal*

**ABSTRACT:** This paper covers the seismic behaviour modelling and numerical analysis of two church structures on Pico Island, Azores, affected by the Faial earthquake on July 9, 1998. The observed damages are first described and some modelling options for the analysis are discussed, particularly in what concerns the way of including the roof as a means of bracing the bearing walls. Frequencies and vibration modes are analysed and discussed for the different types of modelling. Seismic calculations are performed considering the actually recorded accelerograms of that earthquake, and the obtained results are compared with the observed structural damages, in order to propose suitable strengthening techniques based on a better understanding of the structural aspects most directly responsible for the damages. In this context, analysis and discussion are included concerning the influence of modelling type on the peak principal stresses and their zones of occurrence. By comparing those results with the actual damages, it is possible to assess the realism of the modelling hypotheses and then infer which one is most suitable. Based on those conclusions, some strategies are proposed to rehabilitate and strengthen the two churches' structures.

**Keywords:** Modelling, heritage, damages, reinforcement, seismic analysis

## 1 GENERAL INSTRUCTIONS

Many churches have been built as a means to coming closer to God. In a land plagued by so many catastrophes that perhaps no generation has been left untouched, it has always been very comforting for the islanders to have a nearby temple as a place of welcoming refuge. This sentiment was voiced by Fr. Idalmiro Ferreira (Ferreira 1996) *"The complexity of life's problems is so depressing that it need not be further burdened with the baneful thesis of natural fatalities deemed as punishment from above. According to medieval theocentric doctrine, the inexpressible gift of freedom and even the very laws of nature had no effect on the scale of responsibilities attributed to the development of events. In this context, any human misfortune, including natural catastrophes, were viewed as purely and simply the fruit of God's implacable justice."*

These churches are of great importance to the population and to the region's heritage, thereby making the study on the seismic behaviour of their structures an issue of undeniable interest. In cases of earthquake damages – such as those occurred in the churches of Madalena and Bandeiras wards, on Pico Island, Azores – there is technical and

scientific interest in comparing those damages with those estimated through numerical simulation of the structural response to earthquakes that actually occurred in that region.



a) Bandeiras church



b) Madalena church

Figure 1. General view of the churches.

In fact, this comparison may provide important findings about the causes of the damages and allow for a better and properly oriented selection and definition of structural strengthening measures to be implemented.

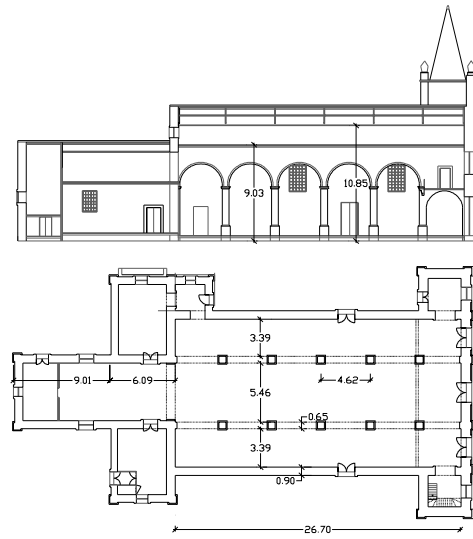
The above-mentioned sets out the framework of the study presented herein, which included an in-depth analysis of the seismic effect on the Bandeiras and Madalena churches. At this stage the work is essentially numerical, but since experimental calibration is essential, an *in situ* campaign of dynamic characterisation tests has already started, aiming at providing sustained estimates of the global structure stiffness parameters. The results of such experimental study have not yet been processed to obtain valid conclusions, but they will be published later, together with any necessary adjustments to the numerical analysis described in this paper.

## 2 DESCRIPTION OF THE CHURCHES AND OF THEIR STRUCTURES

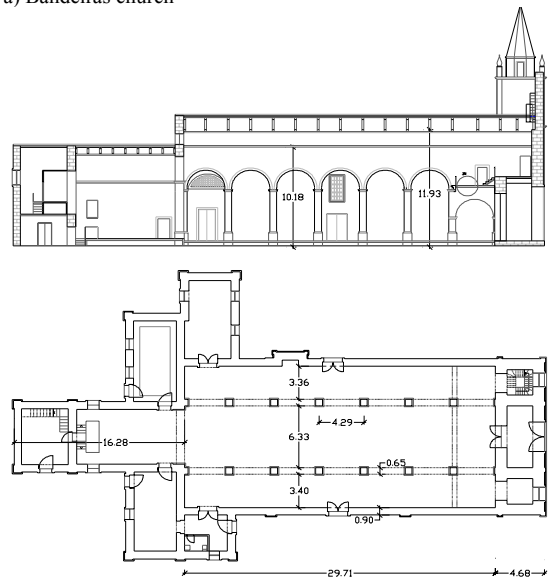
The churches under study are two beautiful neoclassic buildings shown in Figure 1. The Bandeiras church (Fig. 1a) was built in 1860 in the Bandeiras ward which, according to Tomaz Duarte Jr. (Duarte 1999), dates from 1637. According to the same author, the Madalena church (Fig. 1b) was likely “founded in honour of Saint Maria Madalena” in the 15th century. Later, in the mid-17th century, when the population increased, the “primitive” church was replaced by a new building. The new church was built over the old one facing the seaport. Except for some interior and exterior ornaments, particularly the frontispiece, the structure built in the 17th century (Duarte 1999) is the same as the one now found in the ward of Madalena on Pico Island, its facade having been completed in 1891 when the frontispiece was finished.

The churches are similar and consist of three bodies, as illustrated in Figure 2: The first body is the main entrance, including the entrance atrium, the upper choir and the two flanking towers; the second is the main body and consists of three longitudinal naves; the third, the head, consists of the main altar and the lateral and end sacristies.

The churches are also structurally similar, both consisting of walls, arches and columns, a wood frame roof and the upper choir floor over the main entrance area.



a) Bandeiras church



b) Madalena church

Figure 2. Geometry of the churches. Layouts and longitudinal sections

The exterior walls are made of two masonry leaves, with a total thickness of 0.90m, and are the main structural elements. The gabled roof is covered with regional clay tiles placed on a lining supported by a wood frame resting on those exterior and interior walls (of the arches).

### 2.1 *Bandeiras church*

The church has an almost symmetrical shape in relation to the main nave’s longitudinal axis, with minor differences in the lateral sacristies, as shown in Figure 2a. The main body consists of three

naves, one central nave and two side naves, respectively with transversal spans of 5.46m and 3.39m, and a head. The three naves occupy an area of about  $13.60 \times 26.70\text{m}^2$  and the head is 8.63m long up to the altar and 5.64m wide, comprising the lowest and narrowest zone as is common in almost all churches; the head has lateral sacristies on either side.

Each side nave's vault is supported by the exterior wall and by arches over central columns spaced at 4.62m, with  $0.65 \times 0.65\text{m}^2$  cross-sections made of stone. These arches are 9.03m high at the middle of the span and also support the central nave's vault whose crowning is 10.85m high (see Fig. 3). The entrance has an upper choir supported by the exterior walls and by two lower arches, next to which are the towers with exterior dimensions of  $5.10 \times 4.28\text{m}^2$  and an overall height of about 17.0m.

Behind the altar there is a small sacristy with an irregular plasterwork wall (see Fig. 4); in this zone the beams supporting the rafters are placed in a direction contrary to what is normally found in the island's roofs, for which it is presumable that there may exist a transversal wall connecting the longitudinal walls in the altar area.

## 2.2 Madalena church

Madalena church's main body (Fig. 2b) consists of three naves, a central nave with a 6.33m transversal span and two lateral naves with spans of 3.40m and 3.36m, occupying a total area of  $14.5 \times 29.71\text{m}^2$  which does not include the entrance atrium area that is 4.68m long in the longitudinal direction. Each lateral nave is supported on the exterior wall and on arches that are supported by central columns of  $0.65 \times 0.65\text{m}^2$  cross-section and at 4.29m intervals.

These arches support the central (Fig. 5a) that is 10.18m high. The entrance has an upper choir over the entrance atrium (Fig. 5b), connected to two rooms on each of the sides (south and north) of the church's axis. The head, which is 16.28m long and 5.60m wide, is the lowest and narrowest area; and there is a sacristy on each side of the head.

Like in the other church, the structure is nearly symmetrical and also has minor differences in the sacristies. The main facade faces west, and like the towers, is covered in white tiles. The towers, with an exterior dimension of  $4.50 \times 4.50\text{m}^2$ , are part of

the church's nave and have a total height of about 17.20m, excluding the respective roofs that are octagonal. Each nave has an inner vaulted ceiling made of curved sheets of latticed stucco and is illustrated in Figure 5c.



Figure 3 Arches supporting the lateral and central naves



Figure 4 Aspect of the roof over the sacristy behind the altar



a) Nave support arches

b) Central nave and upper choir



c) Ceiling framework

Figure 5. Interior view of Madalena church.

The exterior walls are plastered with cement mortar of good quality. However, an analysis of bore samples revealed that the walls are made of very

irregular material of poor quality, probably due to construction throughout various periods. The plaster itself consists of various layers and incorporates pieces of various materials (tile, bricks, stones, etc.) that fill voids.

### 3 DETECTED DAMAGES

Earthquake damages found on the two churches are directly linked to the type of masonry and to their structural configuration. These damages are described and interpreted in the following sections for each of the two churches.

#### 3.1 *Bandeiras church*

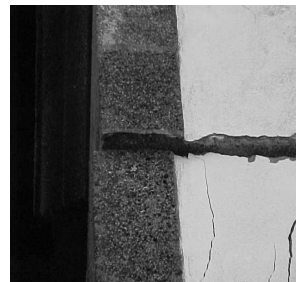
In the Bandeiras church there were found and recorded the following damages. Cracks in the main facade, practically symmetrical in relation to its central vertical axis, with slightly more pronounced damage on the right side, possibly due to ground settlement caused by the earthquakes. There is also a horizontal crack running across the frontispiece about halfway up and that propagates upward.

There is significant cracking in the towers. In the connection between the frontispiece and the tower, the above-mentioned crack extends to the right tower and runs around it, as shown in Figure 6a. The bell tower suffered great damage, with cracks running from the openings to the corners (as illustrated in Figure 6b) and substantial sliding between stones (Fig. 6c).

In the exterior, other cracks were detected, of which two particular examples may be seen in Figure 7, located in the towers' connection to the church body (Fig. 7a) and at the top of the right lateral external wall, between the windows and the coping (Fig. 7b). This last crack is also visible in the interior, as shown in Figure 8a; cracking was also found in the transition between the main body and the chancel (more specifically, next to the keystone of the triumphal arch) and in the area where the longitudinal walls connect to the upper choir and the towers. The arches providing access to the towers show evident signs of movements (Fig. 8b), with settlement in the area of the respective keystones. Finally, the ceiling lining above the upper choir was found ruptured, possibly caused by falling stones.



a) Cracks around the towers b) Cracks in corners



c) Sliding of stones  
Figure 4. Damages in the towers.

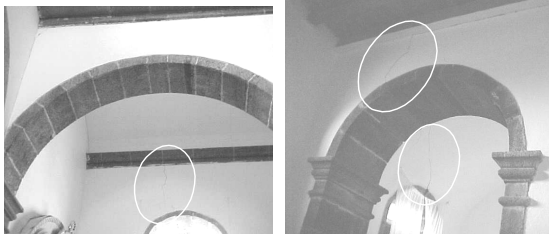


a) Cracking in the connection tower – lateral wall  
b) Crack in the lateral wall over the window  
Figure 5. Damages on the lateral wall.

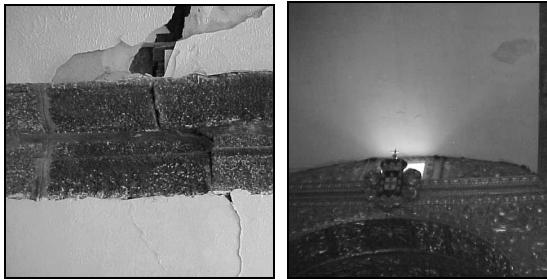
#### 3.2 *Madalena church*

Although a visual inspection revealed that the Madalena church was less damaged than the Bandeiras church, the following failures were nonetheless detected:

1. Some wall tiles fell from the towers and from the main facade, and the pinnacle also fell from the top of the right tower.
2. Substantial cracking in the exterior, in the body of the church's north end, and a vertical crack along the stone over the church's north side door.
3. Interior cracking in the upper choir area, specifically where the towers connect to the nave (Fig. 9a); the central nave's vaulted ceiling sagged slightly, causing the mortar to loosen, particularly next to the triumphal arch (Fig. 9b); loosening of stucco in various places on the ceiling of the naves (Fig. 9c).



a) Crack between the windows and the coping  
 b) Crack in the access arches  
 Figure 6. Examples of damages inside the church.



a) Cracking on the upper choir  
 b) Slight ceiling sag



c) Stucco fell from the ceiling  
 Figure 7. Damages detected at the Madalena church.

#### 4 NUMERICAL SIMULATION OF THE STRUCTURAL SEISMIC BEHAVIOUR

The aforementioned damages reveal major structural movements in both buildings under analysis, which were simulated using appropriate numerical modelling. Although performed within the context of elastic linear behaviour, the numerical simulations showed stress concentration zones (and possible local rupture) and also allowed for the estimation of the stress levels on the structural materials.

##### 4.1 *Structural modeling and mechanical characteristics*

The structures of both churches were discretized through the finite-element method using the

CASTEM2000 program (CEA 1990). Three-node shell elements were used to model the walls, and two-node bar elements for the wood rafters and beams. All structural parts that could affect the structural behaviour of the churches were modelled. The following three simulation hypotheses were assumed as schematized and illustrated in Figures 10, 11, and 12:

– Model A – the structure was considered in a manner that allowed the attempt to reproduce a situation similar to that existing prior to the earthquake of July 9, 1998, where, since the roof rafters and beams were not sufficiently connected to the walls, the walls were not braced along their tops and therefore mainly behaved as cantilevers (Figs. 10a, 11a, and 12a).

– Model B – due account was taken for possible wall bracing provided by the rafters (or other elements) at the top of the walls; the roof structure was thus discretized with beam elements to model the rafters and beams that, when properly connected to the walls by metallic devices, may be active under both tension and compression (Figs. 10b, 11b, and 12b).

– Model C – the roof was assumed with substantial in-plane stiffness, therefore with the capacity to behave as a diaphragm at the roof level, and also connected to the walls using lintels over the walls; in this model, considered only for the Bandeiras church, the discretization was made with shell elements also in the roof (Figs. 10c and 11c), through which it is expected to simulate a hypothetical reinforcement using a thin slab of reinforced microconcrete over the wood lining.

As for the materials, physical properties (specific mass  $\rho$ ) and mechanical parameters (elasticity modulus  $E$  and Poisson coefficient  $\nu$ ) were adopted with the values described in Table I and in accordance with test results described in Costa (1999). Note that, for the roof as simulated using model C, the average mass and elasticity modulus values were computed for a mixed structure of wood with a thin concrete slab, including the roof tile as part of the mass. In model A, the roof mass (wood and tile) was included through additional masses in the walls' top contour nodes.

For each of the indicated modelling hypotheses, the frequencies and respective vibration modes were obtained in order to assess the sensitivity of the main characteristics of dynamic structural response and to compare them among the various modelling assumptions.

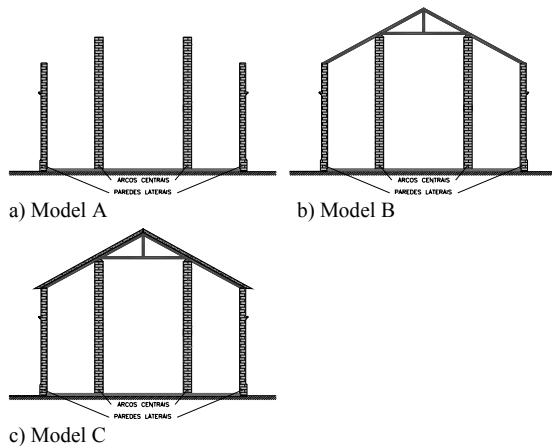


Figure 8. Models taken into account.

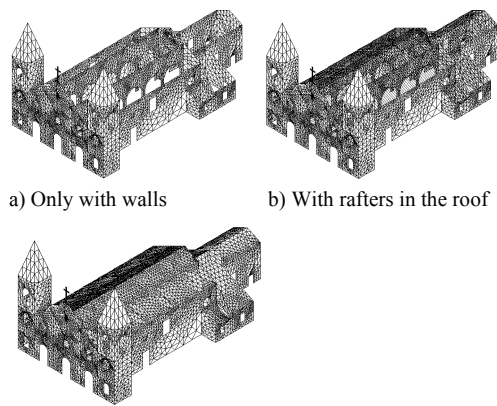


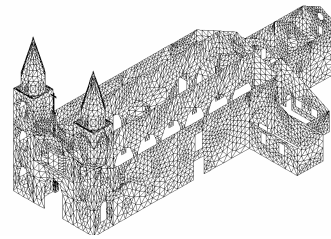
Figure 9. Finite elements mesh used in the structural modeling of the Bandeiras church.

Table I. Material properties.

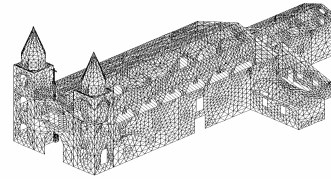
Element	Material	$\rho$ ( $\text{ton}/\text{m}^3$ )	$E$ ( $\text{GPa}$ )	$\nu$
Walls	Stone masonry	1.8	0.4	0.2
Rafters	Wood	0.4	2	0.2
Roof (model C)	Wood and mortar	2.7	25	0.2

#### 4.2 Seismic action and structural response

Seismic load was characterised by accelerograms recorded on July 9, 1998, at the foundations of the Prince of Monaco Observatory, located in the Horta town, Faial Island, and about 10 to 15km from the epicentre. The three components of the referred seismic record (Fig. 13) were taken into account, showing a peak acceleration value very close to  $400\text{cm}/\text{s}^2$  in one of the horizontal components.



a) Only with walls



b) With rafters in the roof

Figure 10. Finite elements mesh used in the structural modeling of the Madalena church.

Figure 13 also includes the corresponding power spectra, from which it was found that the recorded horizontal components (XX and YY) are richer in the frequency range between 1 Hz and 2.5 Hz, whereas the vertical component (ZZ) is more intense, from 6 Hz to 7 Hz. In this study, the YY direction was regarded as coinciding with the church longitudinal axis, such that the earthquake most damaging component (XX) acted in the direction that was found to be the most vulnerable for the structure.

These seismic records reveal an aspect that may have affected the structural response of masonry stone. In fact, during the first instants of earthquake activity (up to about 3s) the vertical acceleration component reached very high values (about  $3.2\text{m}/\text{s}^2$ ), whereas the horizontal component did not exceed half of that value.

Therefore, the vertical acceleration may be responsible for prior loosening of the filling material of masonry walls and for some destruction of internal stone interlocking that is essential for masonry resistance to horizontal actions. After this effect, there occurred intense horizontal acceleration peaks that became more potentially destructive for the wall internal “microstructures” which were weakened in the meantime and whose resistance depends on friction mechanisms caused by gravity loads. In the authors’ opinion, this was one of the aspects likely to have caused serious damages to many of the constructions on the Faial and Pico Islands in the earthquake of July 9, 1998, and this is also the reason for taking into account this real seismic record in the numerical study.

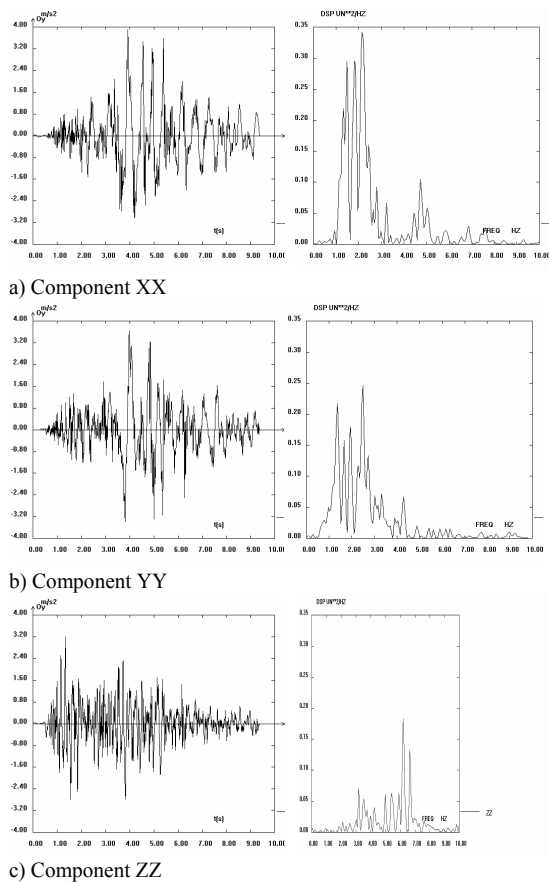


Figure 11. Acceleration's records of the three components of the earthquake on July 9, 1998, and the corresponding spectral power densities.

It must also be pointed out that the referred peak acceleration value of this seismic load is about 2.4 times the Portuguese national code value (RSA 1985) of the peak ground acceleration ( $177\text{m/s}^2$  for soil type I and  $150\text{m/s}^2$  for soil type II) (Ravara et al. 1984). Therefore, if the seismic analysis was to be made for accelerograms with a peak acceleration level corresponding to that code level, expected results could be less than half of those obtained here.

This sort of incoherence between the recorded earthquake and the standard seismic action has however a justification related with the location where the records were taken (the Prince of Monaco Observatory in Faial is at the top of a hill, about 60m high). In fact, previous studies (Escuer 2001), have already reported a "site effect" that amplifies seismic movements up to a magnifying factor of about 2 in the peak amplitudes, which complies with the aforementioned peak

acceleration factor of 2.4 over the code seismic action.

This means that, if the results obtained herein are faced as design indicators, they must be scaled to a level compatible with that of the standard peak ground acceleration. Despite the referred factor, these accelerograms were, nevertheless, used because of the advantage of their real frequency content that reflects the specific features of the site generation mechanisms of earthquakes. If the analysis is done within the linear elastic domain, the scale factor can be directly applied in the results, but, obviously, if a nonlinear analysis is to be made, the accelerogram must be corrected in advance.

The seismic response of the church structure was obtained considering linear elastic behaviour by time domain integration using the Newmark method and taking into account the viscous structural damping according to the Rayleigh formulation, proportional to mass and stiffness. This damping was calibrated to ensure a damping factor not greater than 5% in the frequency range of interest for the horizontal and vertical components, i.e. from 1 Hz to 7 Hz.

Calculations were made to obtain values of all relevant magnitudes, either in time-histories or in terms of maximum values, particularly of displacements, internal forces (of membrane and bending), vertical and horizontal stresses and principal stresses. For the latter, the respective orientations were also obtained in several walls that were suitably individualised for ease of analysis.

## 5 DYNAMIC AND SEISMIC RESPONSE ANALYSIS

For the Bandeiras church, a comparative analysis was made concerning the structural vibration modes and frequencies, as well as the envelopes of principal stresses resulting from the seismic analysis. The three aforementioned modelling assumptions were considered, aiming, on the one hand, to check which situation fitted better with the observed behaviour and, on the other hand, to assess which one performs better within the perspective of seismic strengthening. Based on the conclusions of the Bandeiras church study, the results for the Madalena church are also presented and discussed. Since the study focuses on an actual reinforcement proposal, the results are basically analysed for the case of using a roof

model with rafters (model B) properly connected to the walls, because the envisaged strengthening solution is based on stresses determined from that configuration. However, and where relevant, some specific comparisons are made with the results of modelling assumption A.

## 5.1 *Bandeiras church*

### 5.1.1. *Vibration frequencies and modes*

For each modelling hypothesis, Table II presents some of the first vibration frequencies of certain types of vibration modes, and also provides an abbreviated description of the main structural elements involved in the respective deformation; in some cases, detail is also given for the type of deformation (e.g. 1c = simple curvature bending; 2c = double curvature bending; sym. = symmetry; antisym. = anti-symmetry). Figure 14 shows the first modes corresponding to each modelling hypothesis, in plan view and perspective. By interpreting Table II and through a detailed observation of the corresponding vibration modes, the following considerations can be made:

- The first modes always involve the arches and also mobilise the exterior longitudinal walls for the roof model with rafters. As expected, frequencies increase when the simulation includes structural roof elements (rafters or a thin slab of microconcrete and wood) with an effective connection to the supporting walls and arches.
- In the model without a roof, there is a wide number of modes (except for the first two) fitting in the frequency range of 1 Hz to 2.5 Hz, in which the earthquake horizontal components are more damaging. Those modes range from the 3<sup>rd</sup> to the 14<sup>th</sup> mode, involving the nave arches, the exterior longitudinal walls, the towers and the frontispiece, where in fact there were substantial damages.
- Adding rafters in the simulation forced the nave arches and exterior longitudinal walls to act in combination, such that the 1<sup>st</sup> and 2<sup>nd</sup> modes have now much higher frequencies and fitting within the more unfavourable range. However, the greater arch stiffness resulting from the rafter bracing reduced the number of modes within the critical range (from about twelve to eight modes) and called for the participation of other structural elements such as the altar arch. However, the elements where the worst damage was caused contribute to the vibration modes that fall within the critical range.

By considering the roof structure with a thin slab of microconcrete and wood rigidly connected to the nave wall and arches, frequencies become significantly increased such that only three vibration modes have frequencies within the critical interval. However, these modes still involve arches, exterior longitudinal walls and towers, and have configurations suggesting that those elements are subject to high stress. In this case, the front wall and the frontispiece appear only in higher modes, already outside the critical zone.

Table II. Frequencies obtained in the various models.

	Mode No.	Freq. (Hz)	Element (Deformation)
Model A (without roof)	1	0.538	Arches (1c)
	3	1.228	Arches (2c)
	5	1.285	Lat. wall (1c) Arches (2c)
	7	2.102	Lat. wall (2c) Arches (3c) Frontispiece Towers
	11	2.25	Lat. wall (2c) Arches (3c) Frontispiece Towers (sym.)
	12	2.364	Lat. wall (2c) Arches (3c) Frontispiece Towers (antisym.)
	14	2.494	Lat. wall (2c) Frontispiece Towers (sym.) Arches (3c)
Model B (with rafters)	1	0.963	Wall and Arches (1c, antisym.)
	2	1.278	Wall and Arches (1c, sym.)
	3	1.765	Arches (2c)
	5	2.149	Frontispiece Arches (2c) Altar arch
	8	2.343	Towers
	15	3.191	Frontispiece Towers (torsion)
	18	3.697	Altar wall
	24	5.933	Frontispiece Towers (sym.)
Model C (with thin slab)	1	1.915	Arches (1c)
	3	2.365	Wall (1c) Arches, Towers
	4	2.632	Arches (2c)
	6	2.715	Towers Arches (antisym.)
	8	2.948	Towers Arches (sym.)
	15	4.472	Front wall Choir, Towers Arches (sym.)
	24	5.933	Frontispiece Towers (sym.)

### 5.1.2. *Maximum principal stress values*

The maximum principal stresses, positive (tensions) and negative (compressions), are listed in Table III for the three modelling hypothesis taken into account (A, B, and C) and for four zones selected

as the most representative of structural behaviour: the main facade (including the three entrance arches and the frontispiece), the towers, one of the longitudinal lateral walls (the right one) and one of the nave's row of arches (also on the right side). Table III indicates maximum values (in absolute value) of tensions or compressions extracted from the interior and exterior sides of each wall or set of walls under analysis. The critical zone where those tensions take place is also briefly indicated and shading highlights maximum values for each model.

An overall analysis shows that the maximum compression value (7.95 MPa) is compatible with the compression strength for this type of masonry, although much higher than what is due to gravity load (in this type of structures generally about 1 MPa). As for the maximum tensions (6.23 MPa), they clearly exceed the tensile strength that may be attributed to any stone masonry (and even to common concrete), which indicates the formation of significant cracking as it really occurred in the actual structure.

Also note that in an elastic linear analysis compressions obtained in this way should be less than what could be expected from a nonlinear analysis. In fact, the large tensions obtained show that this study should be adjusted to take into account the nonlinearity associated to the opening of joints between blocks. However that task is foreseen for a subsequent stage of this work, from which there can be expected larger compressions in the referred joints.

The values and the location of stresses obtained for each type of model are next analysed. As already stated, it is worth reminding that model A (without any structure in the roof) is regarded as the closest to the structural reality when the earthquake took place.

*Model A (without roof):*

- The maximum stresses occur in the right lateral wall (longitudinal), and even indicate a tensile stress close to the maximum value obtained in the whole structure, thus agreeing with the vibration modes described in Table II. In fact, vibration mode 7 has a frequency of 2.107 Hz, which is very close to the power spectrum peak frequency of the XX earthquake component (see Figure 13) which is in the normal direction to that wall. Therefore, that mode, involving double curvature horizontal bending of the longitudinal walls, is greatly excited by the said earthquake component and causes large

stresses, particularly where the walls connect to the tower, a location of notorious structural irregularity.

- For the same reason, the walls of the nave arches also have significant stresses, essentially where they connect to the facade wall, although with lower values than in the lateral wall, probably because the wall of arches is less rigid in terms of horizontal bending.

- The towers tend to have lower stresses values, although the maximum tension is significant (4.67 MPa) but possibly because it occurs in the tower's interior wall that connects to the longitudinal lateral wall.

- Finally, the main facade is the least critical of the four zones under analysis. This may be related to the fact that the first vibration mode under which that wall begins to deform (mode 7) – despite being the mode that also causes serious effects on the longitudinal lateral walls and on the arches – is not significantly affected by the YY component of the earthquake that would be the most damaging component for the main facade (and in particular for the frontispiece).

*Model B (roof with beam elements):*

- Peak stress values still occur in the lateral wall, particularly in its connection to the tower, although with decreased tensions and increased compressions.

- There are lower stresses in the arches and in the main facade (more significant in tensions in the arches) compared to stresses obtained in model A. The maximum values of tensions on the arch walls occur at the base of the central columns.

- The towers are the elements with the lowest stresses, although there are significant values due to deformation compatibility where they connect to the facade wall. This is in accordance with the fact that the first vibration mode involving the towers has a frequency (2.343 Hz) already above the peak frequency of the earthquake's power spectrum (about 2.1 Hz) and is therefore excited with much less intensity.

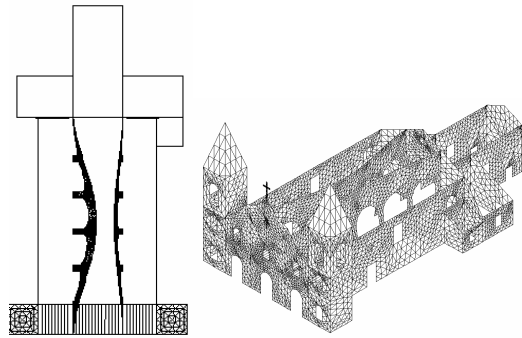
*Model C (roof with shell elements):*

- The maximum stresses (tension and compression) take place in the central nave's wall of arches, particularly in the base of the central columns, because the first two vibration modes have frequencies close to those of the power spectrum peak and essentially involve that wall with a predominance of vertical bending. The in-plane roof stiffness restricts the horizontal longitudinal bending of the wall of arches as

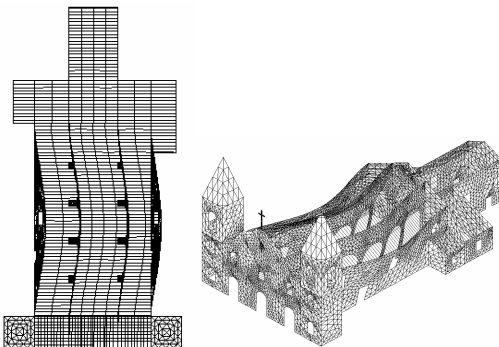
illustrated in the comparison of the first vibration modes in models A and C (Figs. 14a and 14c).

– The main façade and the towers showed lower stresses because they are less involved in the vibration modes within the earthquake critical range of frequency.

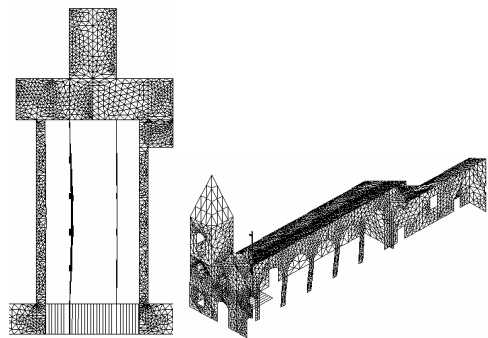
In the lateral wall a substantial decrease is detected in maximum stresses because the respective lower vibration mode has a frequency (2.365 Hz) above the peak frequency of the earthquake power spectrum. Moreover, those maximum values are localised in the connection to the towers in a zone already identified as critical.



a) 1st mode (0.538 Hz); Model A



b) 1st mode (0.963 Hz); Model B



c) 1st mode (1.915 Hz); Model C

Figure 12. First vibrations modes for the three models.

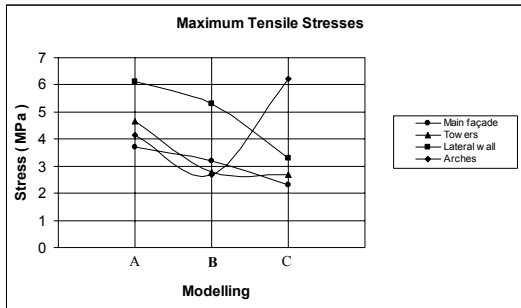
Table III. Maximum principal stresses values obtained with the various models (MPa).

		Model A		Model B		Model C	
		Stress	Critical Zone	Stress	Critical Zone	Stress	Critical Zone
Main Façade	$\sigma^+$	3.71	Connection to the tower	3.21	Connection to the tower	2.30	Connection to the tower
	$\sigma^-$	3.62	Connection to the tower	3.15	Connection to the tower	2.65	Base
Towers	$\sigma^+$	4.67	Int. wall conn. right lat. wall	2.77	Interior wall conn. to façade	2.68	Rear wall conn. lateral wall
	$\sigma^-$	3.13	Interior wall base	2.94	Interior wall base	3.21	Rear wall conn. lat. wall
Right lateral wall	$\sigma^+$	6.12	Conn. to tower	5.30	Conn. to tower	3.28	Conn. to tower
	$\sigma^-$	5.14	Conn. to tower	7.10	Conn. to tower	3.72	Conn. to tower
Arches of right nave	$\sigma^+$	4.14	Faç. connection	2.69	Central base	6.23	Central base
	$\sigma^-$	4.31	Faç. connection	3.50	Central base	7.95	Central base

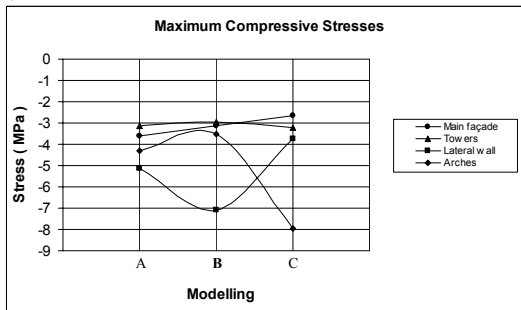
In order to compare the results in each individual zone of the structure, Figure 15 illustrates the maximum value variation obtained for tensile and compressive stresses according to the adopted modelling. The following was found:

- Stress values are reduced in the main façade when the roof is added and this becomes more pronounced when the model includes shell elements. The same is applicable to the towers where the critical tension point is located in the connection to the adjacent walls.
- Tensile stresses in the longitudinal lateral wall decrease substantially when the roof is added. Compressions are also decreased with model C although they increased for model B. In either case, it is always the connection to the tower that is subject to the maximum values.
- Although stresses decrease (particularly tension) in the wall of the nave arches when the roof with rafters is added (which also mobilises the lateral longitudinal walls), the most obvious aspect is the large stress increase at the base of the central columns of the arches when the shell model is applied for the roof. As already indicated, this increased stresses occur because all the vibration

modes of significance in the earthquake critical range show predominant deformation of the arch walls.



a) Maximum tensile stresses



b) Maximum compression stresses

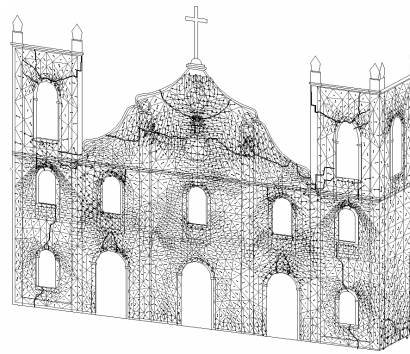
Figure 13. Comparison of stresses of the three models.

According to the aforementioned, model B seems to provide more satisfactory overall results. In fact, tensions always decrease in the four analysed zones and, although they do not decrease as much as in model C (particularly in the main facade and in the lateral wall), what is important is that the larger stresses still persist in a more localised zone next to the tower connection where the overall stability is not at risk. On the contrary, model C, with the most pronounced tension decrease in the facade, towers and lateral wall, nonetheless leads to large stress concentrations at the base of the central arches where the structural overall stability may be at risk and where it becomes more difficult to apply a nonintrusive reinforcement solution that is aesthetically unappealing.

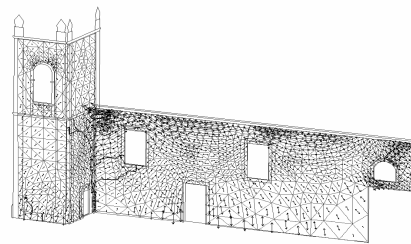
### 5.1.3. Principal stress directions

The pattern of maximum principal stress directions, particularly for tension, allows for the determination of the formation of cracks (perpendicular to the tensile stress directions) in several locations and that may be compared with the real cracks.

Figure 14 shows two perspective views of the patterns of the maximum principal tensile stress vectors determined during the analysis for the whole front wall (including the towers) and for the right side longitudinal wall (including also the lateral rear part of the right side tower).



a) facades and towers



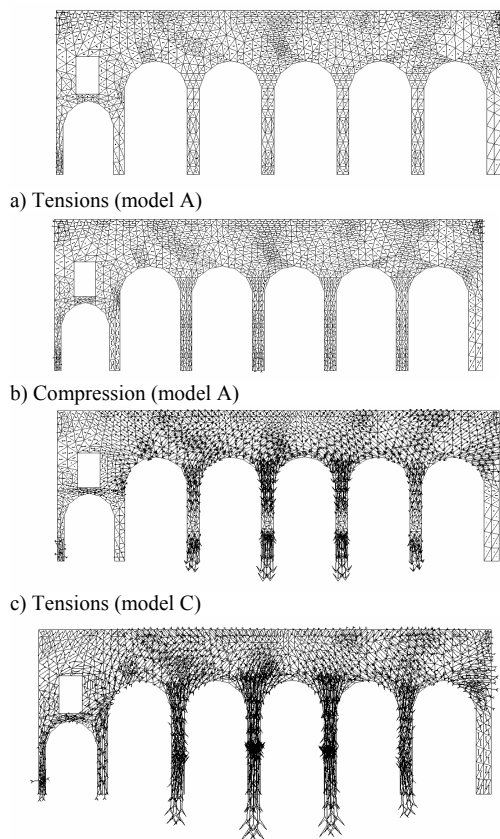
b) Right tower and right lateral wall

Figure 14. Principal tensile stresses directions (model A) and actually detected cracking pattern.

These results refer only to model A (without a roof) since, as already mentioned, it is closer to the real structure. The actually detected cracks in the structure were also plotted in the referred patterns, and it can be seen that the tensile stress vector distributions are denser in the zones surrounding those cracks. Figure 16a, in particular, shows the tension areas where the facade connects to the frontispiece (at the roof level) and in some of the tower and facade arches, whereas Figure 16b refers to cracking in the corner connection between the lateral wall and the tower.

The results, although obtained by means of a linear elastic analysis without a refined discretization of the masonry, do agree fairly with the actually observed damages, thereby validating the confidence in the applied modelling. Finally, Figure 17 also shows the vector field pattern of the maximum principal stress in the walls of the nave arches, for models A and C, respectively.

For model A, some stress concentration was found in the top-ends connecting to the facades and in the bases of arch columns. Switching to model C, it can be noted a significant stress increase, particularly in the arch columns. From this increase, it can be inferred that the columns are subject to vertical bending associated to a fixed-end bending moment in the base that progressively decreases until reaching an opposite sense moment in the column mid-height; this is consistent with the fact that columns are supported on the base and on the roof's shell.



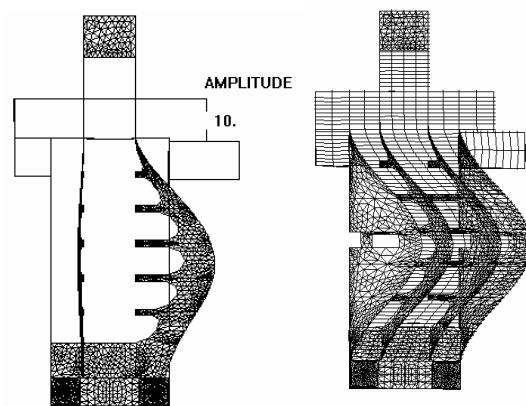
d) Compressions (model C)  
Figure 15. Principal tensile stress directions in the nave arch walls (models A and C).

## 5.2. Madalena church

### 5.2.1. Vibration frequencies and modes

Considering both modelling assumptions A and B for Madalena church, frequencies and vibration modes were computed, the first of which are illustrated in Figure 18.

The first ten frequencies for model A were found to vary from 0.406 Hz to 1.78 Hz, the corresponding vibration modes being symmetrical and antisymmetrical, two by two, and associated to the vibration of exterior walls and of interior arches. All those modes involve bending of the exterior and interior walls that are supported on the base and on the nave ends (sacristy body and entrance area). In the 7<sup>th</sup> vibration mode (with a frequency of 1.638 Hz), corresponding to the 3<sup>rd</sup> mode of the interior walls and to the 2<sup>nd</sup> mode of the exterior walls, the towers follow the mode of the exterior walls.



a) Modeling with only walls ( $f = 0.406 \text{ Hz}$ )  
b) Modeling with roof rafters ( $f = 0.76 \text{ Hz}$ )  
Figure 16. 1st vibrations modes of the Madalena church.

Concerning the model B, frequencies increase such that the first ten values vary from 0.76 Hz to 2.48 Hz; this is due to the increased structural stiffness of walls, which now have also a support at their top-end. The corresponding vibration modes show combined deformation of the exterior walls and of the nave arches, which are symmetrical and antisymmetrical modes, two by two. In this case, since the walls are stiffer and the respective vibration modes occur for higher frequencies, it is also noted that the overall and tower modes are associated to those of the walls. The 1<sup>st</sup> mode layouts, shown in Figure 18 for each of the modelling hypotheses, confirm the aforementioned aspects.

### 5.2.2. Analysis of stresses, internal forces and global displacements

As already stated, tension and stress results were analysed only for model B hypothesis since the reinforcements are studied based on the stresses obtained from this modelling assumption.

By consulting the results for the applied seismic load, and taking into account the observations already made in section 4.2 about the peak acceleration intensity, the following aspects are highlighted:

*Vertical and horizontal tensile stresses* are low in the *main facade*, except in specific points, namely in the frontispiece connection to the towers and in some arches, where values reached 1.69 MPa for horizontal tensions (Fig. 19a), and of 1.70 MPa for vertical tensions. Average values of *vertical compression stresses* (Fig. 19b) were about 1.6 MPa at the wall base, whereas the *horizontal compression stresses* were very low, except in the frontispiece-tower connections where values reached 2.0 MPa. The *vertical moments*, which would correspond to the vertical reinforcement in a reinforced wall, were found with very large values (Fig. 20a) in the zone where the frontispiece connects to the roof and also in the connection to the cross (indicating that the cross must be well connected). The *horizontal moments*, which would correspond to a horizontal reinforcement, reach their maximum values in the frontispiece-tower connection zone (Fig. 20b), whilst the other values are much lower and uniform.

There are low horizontal tensile stresses in *lateral walls* (not illustrated), although a stress concentration zone was detected in the intersection of the exterior wall with the front tower, where tension reached about 3.0 MPa. Similar to horizontal tension and except in the connection to the towers, the *vertical tension* is also low, of about 0.2 MPa.

On average *vertical compression stresses* are low, about 0.5 MPa at the wall base, but there are larger values in *horizontal compressions* at the wall's top-end, next to its connection to the wall containing the altar arch. The *horizontal moments* (Fig. 21a), which would correspond to a horizontal reinforcement, reach their maximum at the top-end of the walls and in the zone where they connect to the sacristy wall and to the interior wall of the triumphal arch; however, large values appear half way along the wall over the vertically aligned door and window. The *vertical moments*, which would correspond to a vertical reinforcement, have maximum values in the middle of the wall (as expected), although there are specific spots where these internal forces increase slightly.

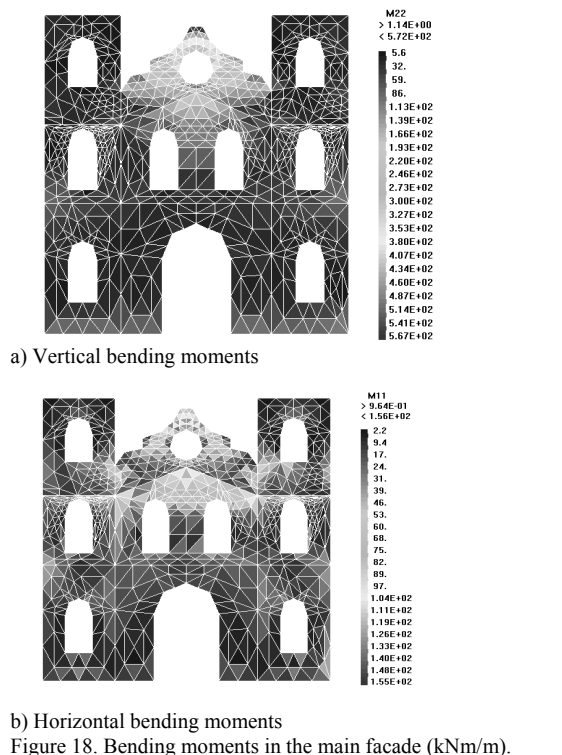
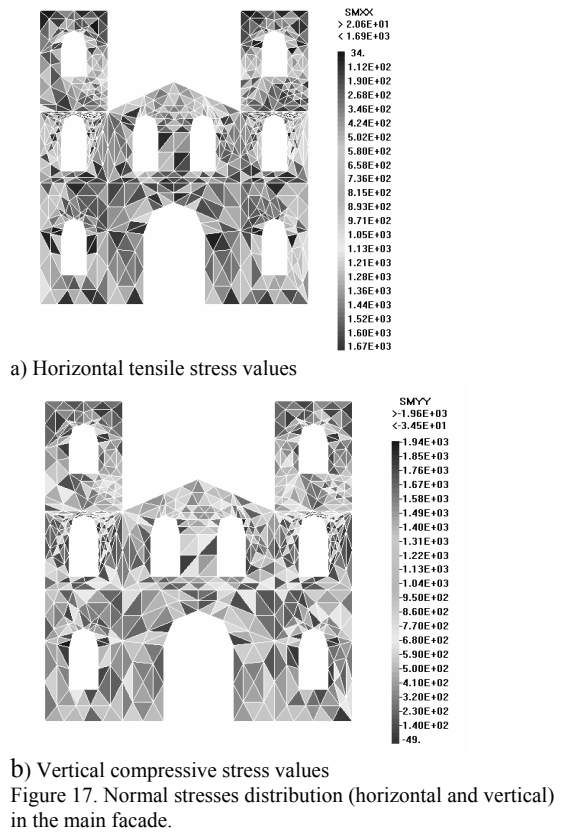


Figure 17. Normal stresses distribution (horizontal and vertical) in the main facade.

Figure 18. Bending moments in the main facade (kNm/m).

The *nave arches* have low *horizontal tensions* where the highest values (1.12 MPa) appear where they connect to the towers and in the arches connecting to the altar arch wall (0.60 MPa). *Vertical tensions* are also low, with the highest values in the 1<sup>st</sup> and 2<sup>nd</sup> arch next to the towers. *Horizontal compressions* are also reduced, the highest values being detected where the nave arches connect to the towers (1.05 MPa) and in the arches next to the altar arch wall (1.00 MPa). *Vertical compressions* reach a maximum value of 1.45 MPa in the first arches associated to the towers. The *horizontal moment distribution* indicates that the arches at the middle of the nave and their connection to the altar arch wall are the zones corresponding to the maximum moments (136 kN.m/m). Finally, the distribution of *vertical moments*, illustrated in Figure 21b, shows that the respective maximum values (175 kN.m/m) occur in the columns of the intermediate arches.

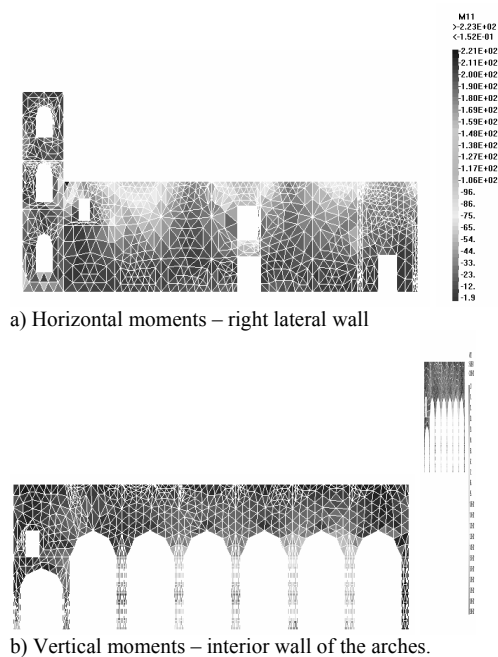


Figure 19. Bending moments in the right lateral wall and in the arch wall.

It is important to note that for model A (without roof rafters), stresses and internal forces are generally about 20% to 30% less than those of model B, the later having been applied for the strengthening study. This aspect makes sense in light of the earthquake frequency content (Fig. 13) and of the fundamental frequencies associated with model A, for which less vibration modes were found within the critical range of the seismic load

(1 Hz to 2.5 Hz), therefore with less sensitivity to that particular action.

Concerning the peak displacement envelope resulting from the applied seismic load, the horizontal deflections were calculated in the direction perpendicular to the walls along the top of the main facade and of the lateral gable. For model A (“without” roof) this resulted in a maximum value of 2.33cm in the main façade and of 1.92cm in the lateral wall. For model B (with rafters in the roof), these values decreased about 15%, respectively, to 2.04cm in the main facade and 1.59cm in the lateral wall (the later, leading to an approximate drift of 0.15%).

## 6 REHABILITATION AND STRUCTURAL STRENGTHENING SOLUTIONS

### 6.1. Introduction

On the Azores islands, seismic actions are the events inducing the greatest loads and causing the strongest damage on most traditional buildings and, in particular, on churches. According to the Portuguese national standards (RSA 1985), the dominant seismic action is of type I, which is usually called a nearfield earthquake, with a relatively high excitation frequency, a short duration and a significantly large vertical component. The earthquake of July 9, 1998, is a good example of that, as shown by the accelerograms and the corresponding power spectra already illustrated in Figure 13.

In buildings essentially made of masonry walls, large vertical accelerations cause serious problems to their structural behaviour because the self-weight effect (as a main element of stabilisation) becomes relieved and allows masonry to disaggregate with relative ease. Therefore, any structural strengthening work must include measures that adequately help the masonry remain intact when subject to intense vibrations, thereby ensuring the integrity of the structural masonry elements.

For masonry constructions to resist seismic events, it is essential that they function as an overall unit. Certainly, a rehabilitation and reinforcement solution must be always based on a compromise between not interfering with the building original design and the need to satisfy safety requirements. However, these measures must be selected and designed to ensure continuity and adequate

connections among all the main structural elements such as walls, floors and roofs, thereby improving the structural behaviour.

The stability of nonstructural elements is another aspect that must be taken into consideration to prevent the occurrence of additional damages to people and goods in their surrounding area. Elements such as entablature, coping, cornices, decorative facades, pinnacles, etc., although not affecting the overall stability of their structural supports, must be carefully analysed and reinforced, even using special connections if necessary. Taking the Madalena church example, it is important to properly connect pinnacles to the remaining structure, and to avoid the sole use of single bars that are unable to provide suitable stiffness and/or structural redundancy to prevent the supported element from falling.

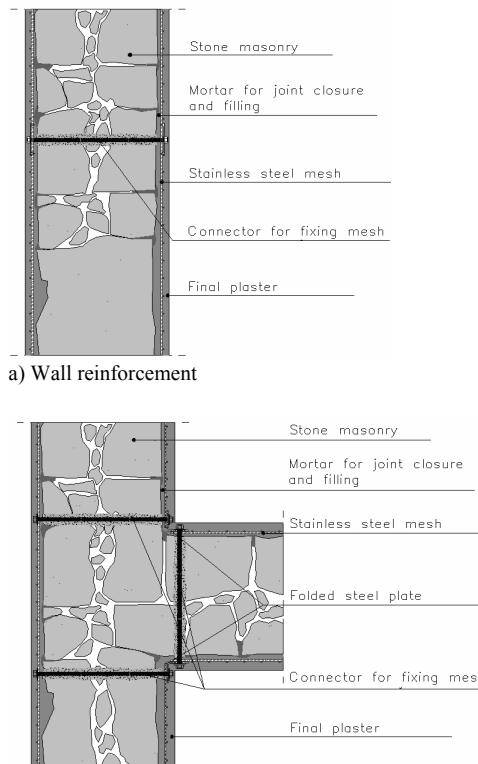
Based on the aforementioned, it is worth highlighting the three main aspects adopted as basic premises subjacent the strengthening schemes for the Madalena church: Prevent masonry, as the predominant structural material, from disaggregating; promote the combined performance of the different structural elements; and ensure the stability of nonstructural parts.

## 6.2. Strengthening schemes

To ensure the integrity of the masonry walls, a good knowledge is first sought of the wall type, which requires giving the walls a thorough cleaning. Since they are double-leaf walls filled with irregular material of varied characteristics, one of the possible strategies is to fill the voids with liquid mortar (Costa 2002) to improve the internal bond of filling material. Whether a simple or double-leaf wall, all joints must be properly closed with mortar made in a 1:3 ratio, part of which should be of volcanic ash to make use of its pozzuolanic properties.

Walls to be plastered, and only these walls, may also be substantially reinforced by including a steel mesh (preferably stainless) on each side of the wall, linked with connectors, as illustrated in Figure 22a. According to Costa (2002), this method will increase the wall resistance by up to 50%. In areas of corners and openings, additional measures must be taken by placing steel folded plates or angle bars bolted to walls (Fig. 22b) whose stones do not intersect properly for good bracing.

Naturally, using these steel meshes in the stone masonry of arches, jambs, and in vertical and horizontal alignments must be restricted and used with precaution to maintain the stone visible. In these cases it will be necessary to use steel elements stitching these corners or intersecting the walls in an oblique direction so that the meshes may be connected. In this type of intervention, it is fundamental that the elevations, particularly the church main facade, remain unaltered.



b) Wall intersection reinforcement  
Figure 20. Wall strengthening schemes.

Floors and roofs may play a fundamental role in the overall structural stability during a seismic event. When considered separately, those elements generally do not need to be reinforced because the earthquake will affect them predominantly in the direction of their greater resistance, i.e. their own plane. However, since floors and roofs should support the lateral walls for adequate horizontal force transfer to the foundation, special care must be taken for enhancing horizontal resistance of those structures. For churches, particularly the two under study, this reinforcement must be planned only for the roof so that, with suitable in-plane stiffness (like a diaphragm), it becomes able to restrict out-of-plane wall movements. This strategy

prevents walls from functioning as cantilevers and forces them to behave as panels supported on the ground and at the roof, as illustrated in Figure 23a.

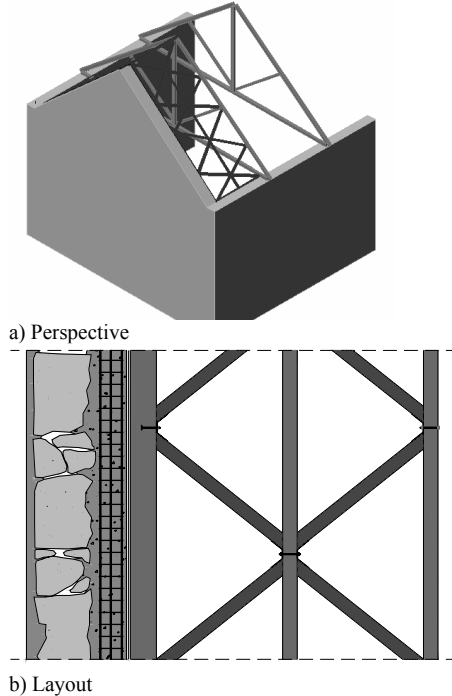


Figure 21. Bracing schemes for a gable end wall.

In the case of an end wall, as shown in Figure 23a, it requires its own bracing at the roof next to the gable, as illustrated in Figure 23b, where it is also highlighted the use of a reinforced concrete tie beam to properly connect the roof to the wall and thus to enhance their combined strength.

Precautions are also necessary in lateral walls where the roof structure is supported. The walls still need to be braced by the roof structure that must be effectively connected to them according to the scheme shown in Figure 24a. In this case, the wall top-end is strengthened with a reinforced concrete tie beam that allows for connecting the wall to the roof structure using bolted steel plates. This beam also provides stability to the wall cornice by connecting it to the beam and to the wall using embedded rods.

The frontispiece, similar to the coping, is a typical nonstructural element that must be stabilised. The frontispiece is an isostatic element supported on the front wall at the coping level and that, due to its dimensions, must be reinforced and properly connected to the towers according to the scheme illustrated in Figure 24b. The proposed

reinforcement of the frontispiece in itself consists of placing steel bars behind it and properly embedded in the masonry wall constituting that nonstructural element.

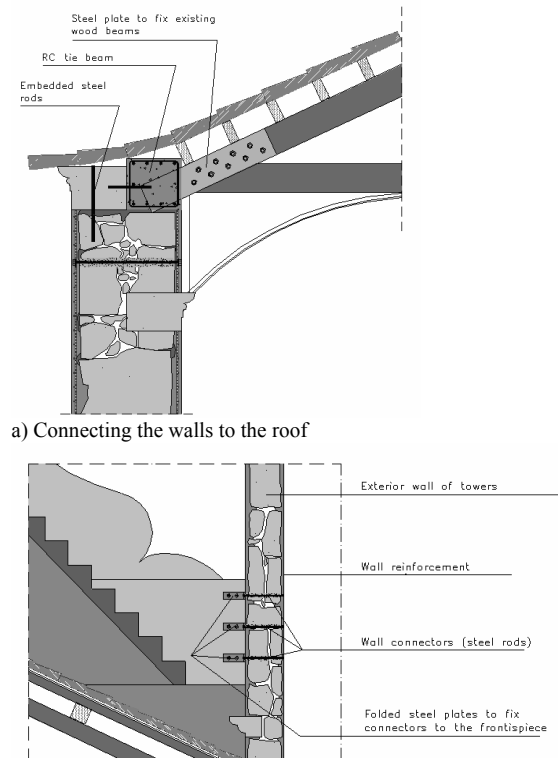


Figure 22. Roof reinforcement schemes.

As already shown, the main facade of both churches has two towers, whose walls are connected to the longitudinal walls of the church nave up to the coping level, above which the tower top part (the bell tower) is connected to the frontispiece. Since they cannot be separated from the nave, the analysis and reinforcement of the towers require special precautions (note that it may be dangerous if the towers detach from the nave, because such a high structure becomes isostatic). Therefore, towers must be reinforced at their bottom part (below the coping) and appropriately connected to the nave. The bell tower must be treated as an independent element, but properly connected to the bottom part at the coping level.

## 7 CONCLUSIONS

This paper briefly described the structures of the Bandeiras and Madalena churches and the main damages detected after the earthquake of July 9, 1998, in the Faial Island, Azores. This information

served as the framework for numerical analysis of the behaviour of those structures taken the real earthquake as the input seismic action.

After a first stage for the definition of geometry and mechanical data of the comprising materials, the dynamic characteristics (vibration frequencies and modes) of both church structures were obtained in order to properly understand their behaviour under seismic actions in general and under the actual earthquake in July 1998.

Time domain dynamic numerical analyses were then performed, taking the input action as determined by the accelerograms recorded during that particular earthquake. This allowed for obtaining maximum internal forces and stresses in agreement with the detected damage, and helped on a proper interpretation of that damage itself. The result analysis suggested suitable reinforcement schemes that were presented for the particular purpose of structural rehabilitation of the Madalena church.

The aforementioned analyses also allowed us to conclude the main aspects summarised in the following paragraphs for each church.

For the Bandeiras church, a comparative analysis was made for stresses resulting from three models: One for the structure as it existed and two other analyses with proposed reinforcement solutions, namely a lighter reinforcement in which the roof wood structure is kept, but with suitable connections to the bearing walls, and another heavier reinforcement requiring that a microconcrete/wood thin slab be incorporated in the roof.

It was found that the roof modification significantly changes the configuration and frequency of vibration modes, and, consequently, the stress values and distributions. Actually, by analysing the principal stresses and respective directions, the structural model without roof (thus, closer to the structural reality when the seismic event occurred) was found to provide results in fair agreement with the observed damages. By contrast, planning a slab in the roof concentrates and increases undesirable tensions in the columns of the nave arches, although significantly reducing stresses in most other elements. The model with a lighter roof, using only wood elements properly connected to the walls, shows overall more satisfactory results, with moderate and generalised decreases of tensile stresses without any particular concentration in

critical zones likely to compromise the overall stability.

Although the nonlinear structural behaviour was not yet taken into account, and which appears to be important in view of the tensile stresses herein obtained with linear elastic properties, this study contributed to a better understanding of the seismic behaviour of these structures. The study also made it possible to compare the performance of two reinforcement solutions that are frequently proposed for these types of buildings.

In the case of the Madalena church, the study focused mainly on an actual strengthening solution. Therefore, following the study for the Bandeiras church and in view of their structural similarities, reinforcement solutions were studied on the basis of the structural response obtained through a model that includes a roof with its rafters properly connected to the walls and that simulates the type of reinforcement best adapted to this type of construction.

In this way a solution was drawn that, in a minimalist manner, would give the Madalena church structure sufficient seismic resistance to withstand other future earthquakes and to continue performing the functions for which it was built and reinforced.

## 8 REFERENCES

- CEA (1990). CASTEM 2000, Guide d'utilisation, CEA, France.
- Costa, A. 1999. *Ensaios de Caracterização de Alvenarias Tradicionais*. ISBN: 972-98312-0-3. Published by M.M. – Trabalhos de Engenharia Civil, Lda, Oporto.
- Costa, A. 2002. *Determination of mechanical properties of traditional masonry walls in dwellings of Faial Island, Azores*. Earthquake Engineering and Structural Dynamics, July 2002.
- Duarte Jr., T. 1999. *O Concelho da Madalena – Subsídios*. History Notes. Published by the Town Council of Madalena, Pico Island, Azores.
- Escuer, M., Dessai, P. & Oliveira, C. S. *Estudo da Amplificação das Ondas Sísmicas no Monte das Moças (Horta, Faial) e Mecanismos Focais Através das Réplicas do Evento de 9 de Julho de 1998*, Sismica 2001 – 5<sup>th</sup> National Meeting of Seismology and Seismic Engineering, Azores, 2001.
- Ferreira, I. 1996. *Convento de S. Pedro de Alcantára. Mosaicos da sua História*. Published by the Ward Council of S. Roque do Pico, Pico Island, Azores.
- Ravara, A., Duarte, R.T. & Carvalho, E.C. 1984. *Engenharia Sísmica de Pontes*, ICT, Specialisation and Improvement, Structures. S318, LNEC, Lisbon.
- R.S.A. 1985. Regulamento de Segurança e Acções para Estruturas de Edifícios e Pontes (National Code Standard of Safety and Actions for Structures, Buildings and Bridges), Imprensa Nacional Casa da Moeda, Lisbon.